SMiRT-12 / K. Kussmaul (Editor)

BG12/5

A FINITE ELEMENT ANALYSIS OF STABLE CRACK GROWTH IN INHOMOGENEOUS MATERIALS

N. Miyazaki[1], M. Nakagaki[2], T. Sasaki[3] and T. Sakai[1]

[1]Department of Chemical Engineering, Kyushu University, Japan
[2]Department of Mechanical System Engineering, Kyushu Institute of Technology, Japan
[3]Kawasaki Heavy Industries, Ltd., Japan

ABSTRACT

The finite element method was applied to generation phase analyses for stable crack growth in inhomogeneous materials. Experimental data on stable crack growth in bimaterial CT specimens, which were composed of a base metal and a weld metal, were numerically simulated using the node-release technique, and the variations of the fracture mechanics parameters such as J-integral, T^*-integral, $\hat{J}$-integral and CTOA were calculated. The effects of the fusion line and the weld on the near crack fracture mechanics parameters were discussed.

1 INTRODUCTION

The J-integral proposed by Rice (1968) has been extensively utilized in assessing the integrity of flawed structural components which undergo plastic deformation. The J-integral is theoretically valid only for nonlinear elasticity where no unloading occurs. The J-resistance curve is used to characterize crack initiation and small amount of crack growth. In the case of large amount of crack growth, a great deal of unloading occurs around a moving crack tip and the J-integral loses its validity because of path dependence. Atluri et al. (1984) and Kishimoto et al. (1980) proposed new fracture mechanics parameters T^*-integral and $\hat{J}$-integral, respectively, which hold path independence during crack growth.

In practical structural components, fracture often initiates not at a homogeneous region such as a base metal but at an inhomogeneous region such as a weld region. In the present study, the elastic-plastic finite element method was applied to generation phase analyses for stable crack growth in inhomogeneous materials using experimentally obtained load-line displacement versus crack extension curves of CT specimens made of a welding joint. The purpose of the present study is to make clear the effectiveness of various fracture mechanics parameters for stable crack growth in inhomogeneous materials and the effect of fusion line on the fracture mechanics parameters.

2 FRACTURE MECHNICS PARAMETERS

Four kinds of fracture mechanics parameters, that is, J-integral, T^*-integral, $\hat{J}$-integral and CTOA, were used in the present study. Their definitions for the mode I are presented here. The path independent J-integral proposed by Rice (1968) valid only for nonlinear elasticity is denoted for an integral path Γ shown in Fig.1(a) as

(1)

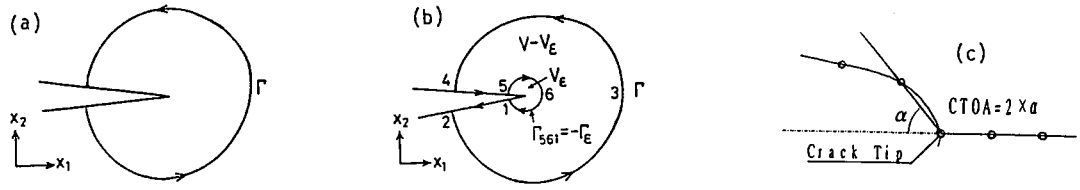

(a) Path for J-integral (b) Path for T^*-integral and $\hat{J}$-integral (c) Definition of CTOA

Fig.1 Integral path and definition of CTOA

where W is the strain energy density, n_1 is the x_1-component of a unit outward normal to the path Γ_ε, t_i is a component of the tractions defined by $t_i=\sigma_{ij}n_j$, σ_{ij} is a component of stresses, and $u_{i,1}$ is a differentiation of displacement with respect to x_1, that is, $u_{i,1}=\partial u_i/\partial x_1$.

Atluri et al. (1984) proposed the T^*-integral, which is valid for arbitrary constitutive relations, arbitrary loading/unloading and crack growth caused by ductile fracture. For an integral path shown in Fig.1(b), the T^*-integral is written in the case of a quasi-static problem as

$$T^*=\int_{\Gamma_\varepsilon}[Wn_1-t_iu_{i,1}]d\Gamma=\int_{\Gamma 12345}[Wn_1-t_iu_{i,1}]d\Gamma-\int_{V-V_\varepsilon}[W_{,1}-\sigma_{ij}\varepsilon_{ij,1}]dV \tag{2}$$

where Γ_ε enclosing a crack tip should be so located in the vicinity of a crack tip as to include a fracture process zone. The physical meaning of the T^*-integral is an energy flow rate into a volume V_ε enclosed by Γ_ε.

The $\hat{J}$-integral proposed by Kishimoto et al. (1980) can be used in the same way as the T^*-integral. For a path Γ_ε shown in Fig.1(b), the $\hat{J}$-integral is written as

$$\hat{J}=\int_{\Gamma 12345}[W_en_1-t_iu_{i,1}]d\Gamma+\int_{V-V_\varepsilon}\sigma_{ij}\varepsilon^*_{ij,1}dV \tag{3}$$

where W_e is the elastic strain energy density, and ε_{ij}^* is a component of strains excluding elastic strains, which are called eigen strains.

As shown in Fig.1(c), CTOA is defined as

$$\text{CTOA} = 2\alpha \tag{4}$$

where α is obtained from the node located at the crack tip and its adjacent node.

3 EXPERIMENTAL DATA ANALYZED AND METHOD OF ANALYSIS

Experimental data on stable crack growth in bimaterial CT specimens were numerically simulated using the finite element method. Four kinds of the CT specimens used in the experiments are shown in Fig.2. The M5G specimen is a homogeneous CT specimen made of a base metal, A533B class 1 steel. Others are SAW welded CT specimens composed of a base metal and a weld metal. In the D5G specimen, a crack is located across the fusion line and an initial crack tip is located in the weld metal. In the F5G specimen, an initial crack tip is located just on the fusion line. In the H5G specimen, a crack tip is initially located in a HAZ and goes across the fusion line. The detailed dimensions are shown in Fig.3 for the D5G specimen. A 20% side groove is machined in all the specimens. An example of the finite element mesh breakdown using 20-noded isoparametric elements is shown in Fig.4 for the D5G specimen, together with the integral paths for the calculation of the fracture mechanics parameters.

The Young's modulus E, the Poisson's ratio ν and the yield stress σ_{ys} for the base metal and the weld metal are as follows (JWES-AE-9004 1990):

Base metal : E = 206.0 GPa, ν = 0.3, σ_{ys} = 550.0 MPa

Weld metal : E = 175.1 GPa, ν = 0.3, σ_{ys} = 630.0 MPa

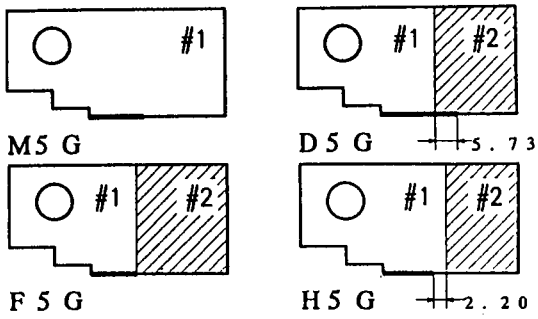

Fig.2 Four kinds of CT specimens (#1:base metal, #2:weld metal)

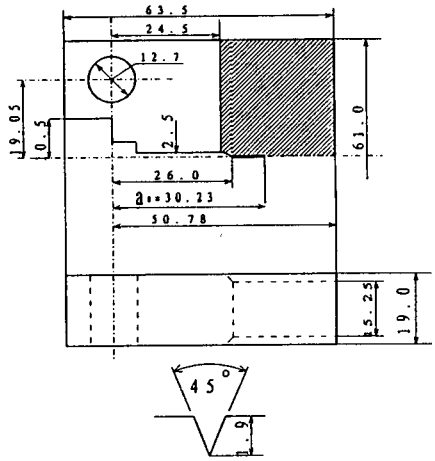

Fig.3 Detailed dimensions of D5G specimen

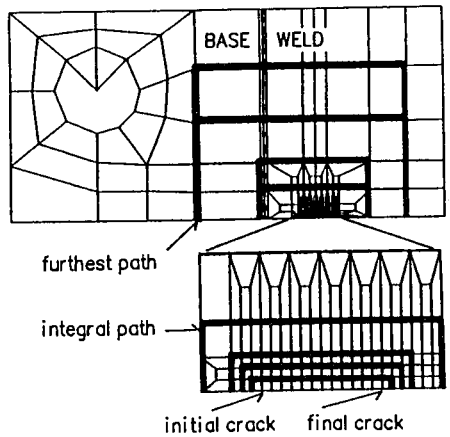

Fig.4 Finite element mesh and integral paths for D5G specimen

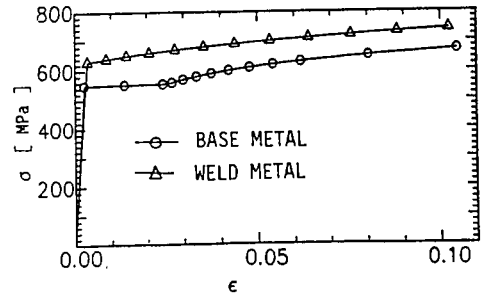

Fig.5 Stress-strain curves for base metal and weld metal

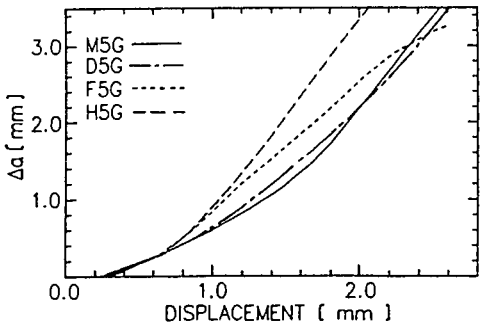

Fig.6 Load-line displacement versus crack extension curves obtained from the experiments

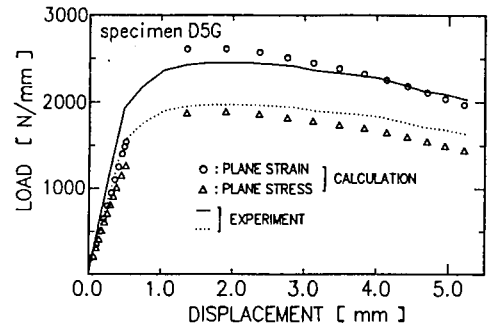

Fig.7 Load versus load-line displacement curves for D5G specimen obtained from the analyses

Experimentally determined uniaxial stress versus strain data for both metals are piecewise linearly approximated as shown in Fig.5 (JWES-AE-9004 1990) and used in the present analyses.

Generation phase analyses for stable crack growth were performed in the present study. Experimentally determined load-line displacement versus crack extension curves shown in Fig.6 were precisely followed in the analyses. The crack tip was extended element by element by unpinning the constraints ahead of the crack tip.

and then the variations of fracture mechanics parameters versus crack extension, that is, fracture resistance curves were obtained from a postprocess code.

4 RESULTS AND DISCUSSION

The tested CT specimens were 19 mm thick. The ASTM size requirement for plane strain condition at the intiation states that:

$$\text{Thickness} > 25J/\sigma_{ys} \quad (5)$$

If we utilize the condition at the proximity of the crack initiation of those tested specimens, say at J = 500 N/mm, the plane strain condition will cease to hold about 1 mm of crack growth. In this reason, the analyses were performed in the plane stress condition and plane strain condition. Figure 7 shows the results of load versus load-line displacement for the D5G specimen. The load from the

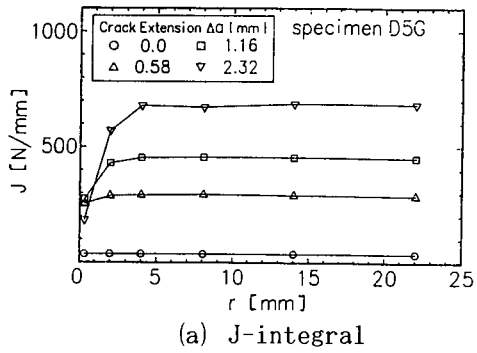

(a) J-integral

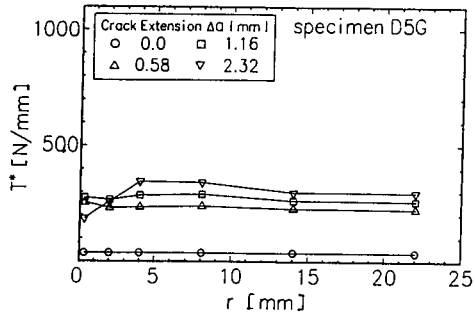

(b) T*-integral

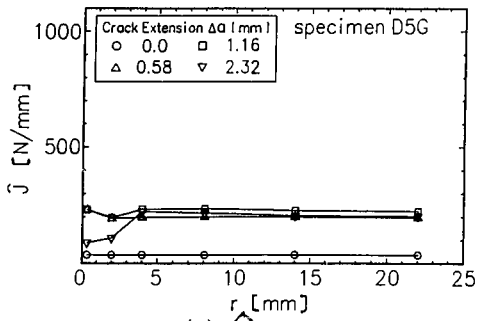

(c) Ĵ-integral

Fig. 8 Path dependence of fracture mechanics parameters

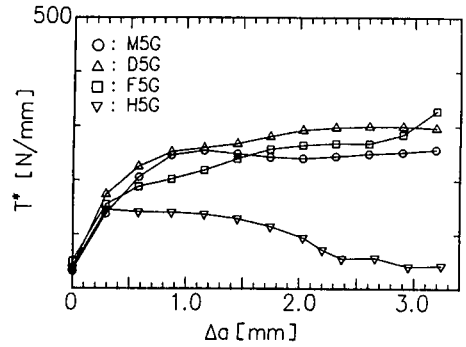

(a) T*-integral

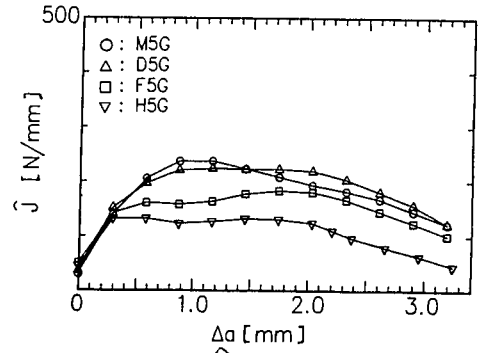

(b) Ĵ-integral

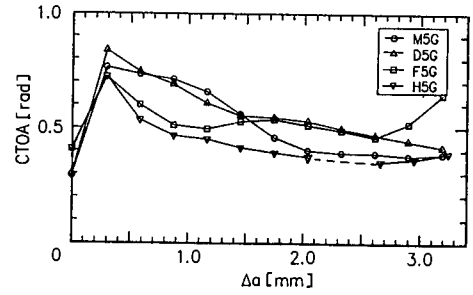

(c) CTOA

Fig. 9 Resistance curve for near crack fracture mechanics parameters

experiment is shown in two folds. The solid curve represents the load normalized by the notch root distance of the side groove and the dotted one represents the load normalized by the full specimen thickness. The fact that the plane strain results agree well with the results of experiments normalized by the notch root distance may indicate that the use of a 20% side groove is appropriate to give rise to the plane strain condition. At the same time, the plane stress results also have a good correlation with the results of experiments normalized by the full specimen thickness. This fact may indicate that the overall behavior of the specimen including the plastic area is close to the plane stress condition. Hereafter we will show the plane stress results for fracture mechanics parameters.

Figures 8(a), (b) and (c) show the path dependence of fracture mechanics parameters for the D5G specimen. The r in the abscissa represents a vertical distance from the crack tip to the integral path. It is seen that after crack initiation, the stress or strain nonproportionality due to the stress unloading emanated from the extending crack tip causes the path dependence of J-integral. So the J-integral value does not represent the severity of the crack tip after crack growth. Compared with the J-integral, the T^*-integral and $\hat{J}$-integral show good path independence.

The summary of the crack resistance over the four specimens are shown in terms of the three near crack fracture mechanics parameters in Figs.9(a), (b) and (c). The three near crack fracture mechanics parameters, T^*-integral, $\hat{J}$-integral and CTOA, have the same overall characteristics of resistance over the four specimens of various crack tip locations with respect to the weld geometry. That is, the crack resistance in the weld metal (the D5G specimen) is slightly higher than that in the base metal (the M5G specimen), or similar. The resistance in the HAZ (the H5G specimen) is apparently lower than the former two. These results are consistent to the Vickers hardness test data on the welded region, as shown in Fig.10 (JWEA-AE-9004 1990), which were measured at the locations of t/4, t/2 and 3t/4 in a welding joint (t:thickness of a welding joint). That is, the hardness as well as brittleness in the HAZ is higher than in the base metal and the weld metal, and the difference between the base metal and the weld metal is small in hardness. In the case where the crack tip is initially on the fusion line (the F5G specimen), the resistance is, for the period of approximately 1.5 mm of crack growth, slightly lower than that in the base metal and the weld metal, then rises to their level. The reason is deduced such that the crack may be still dragging the effect of the HAZ just behind the initial crack tip.

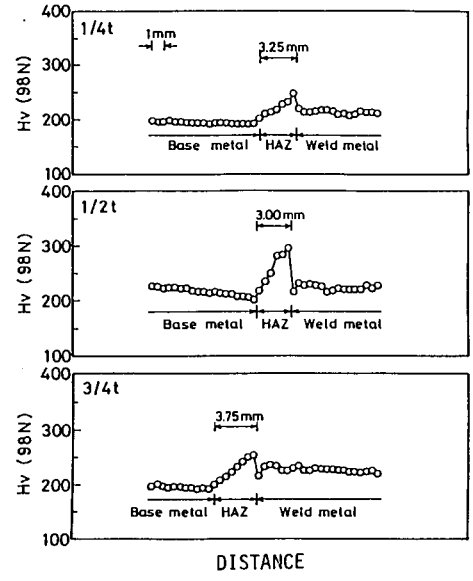

Fig.10 Vickers hardness

5 CONCLUDING REMARKS

The generation phase analyses for stable crack growth in inhomogeneous materials were carried out to calculate the variations of several fracture mechanics parameters. The following conclusions were derived from the present analyses:

(1) The near crack fracture mechanics parameters such as T^*-integral, $\hat{J}$-integral and CTOA can pick up the information on the local brittleness in inhomogeneous material.

(2) When the crack grows in the base metal or the weld metal, clear difference was not found in the crack resistance due to the reason that the difference between the base metal and the weld metal is small in the

brittleness as well as the material properties.
(3) The HAZ, which is more brittle than the base metal and the weld metal, affects the crack resistance represented by the near crack fracture mechanics parameters.

This study was performed under the EPI program, and financially supported by Japanese utilities and fabricators, and USNRC and Martin Marietta Energy Systems, Inc. and Subcontract No.19X-SD561V.

REFERENCES

Atluri,S.N. et al. 1984. Incremental Path-Independent Integrals in Inelastic and Dynamic Fracture Mechanics. Engineering Fracture Mechanics. 20: pp.209-244.

Brust,F.W. et al. 1985. Further Study on Elastic-Plastic Stable Fracture Utilizing the T^* Integral. Engineering Fracture Mechanics. 22: pp.1079-1103.

Brust,F.W. et al. 1986. A Combined Numerical/Experimental Study of Ductile Crack Growth after a Large Unloading Using T^*, J, and CTOA Criteria. Engineering Fracture Mechanics. 23: pp.537-550.

JWES-AE-9004. 1990. Study on Elastic-Plastic Fracture Mechanics in Inhomogeneous Materials and Structures (II). prepared by EPI Subcommittee, Nuclear Engineering Research Committee, The Japan Welding Society.

Kishimoto,K. et al. 1980. On the Path Independent Integral-J. Engineering Fracture Mechanics. 13: pp.841-850.

Nakagaki,M. et al. 1989. Elastic-Plastic Fracture Mechanics Evaluations of Stainless Steel Tungsten/Inert-Gas Welds. in: Nonlear Fracture Mechanics, Volume II - Elastic-Plastic Fracture, ASTM STP 995, edited by J.D.Landes, A.Saxena and J.G.Merkle: pp.214-243.

Rice,J.R. 1968. Path Independent Integral and the Approximate Analysis of Strain Concentration by Notches and Cracks. ASME Journal of Applied Mechanics. 35: pp.379-386.